



International Journal of Sustainable Aviation

ISSN online: 2050-0475 - ISSN print: 2050-0467

<https://www.inderscience.com/ijsa>

Effects of battery degradation on a hybrid electric propulsive system management

Teresa Donateo, Ludovica Spada Chiodo, Antonio Ficarella

DOI: [10.1504/IJSA.2023.10051079](https://doi.org/10.1504/IJSA.2023.10051079)

Article History:

Received:	02 May 2022
Accepted:	30 August 2022
Published online:	06 December 2022

Effects of battery degradation on a hybrid electric propulsive system management

Teresa Donateo*, Ludovica Spada Chiodo
and Antonio Ficarella

Department of Engineering for Innovation,
University of Salento,

Via Per Monteroni, 73100 Lecce, Italy

Email: teresa.donateo@unisalento.it

Email: ludovica.spadachiodo@unisalento.it

Email: antonio.ficarella@unisalento.it

*Corresponding author

Abstract: Amongst the most concerning issues regarding hybrid electric propulsive systems (HEPS), together with sizing and control, is that of energy management strategy (EMS). EMS is crucial for the optimal usage of the system itself and is generally aimed at the minimisation of fuel consumption while keeping under control the battery state of charge, especially if the electric path of the HEPS is also used to ensure power availability in the case of engine failure. However, the battery is prone to fast degradation during its useful life. Therefore, it is particularly important to include battery aging effects in the energy management strategy. The present study compares two different approaches in the energy management strategy of a rotorcraft for urban air mobility, age-dependent and age-independent, on a given mission. The parallel HEPS includes a turboshaft engine, two electric motors, and a lithium battery whose degradation is analysed in terms of capacity, internal resistance, and Peukert coefficient. The results show that the age-dependent strategy determines a more conservative usage of the battery with the consequence of achieving a higher degree of safety at the expense of slightly higher fuel consumption.

Keywords: hybrid electric propulsive systems; HEPS; energy management; battery aging; urban air mobility.

Reference to this paper should be made as follows: Donateo, T., Spada Chiodo, L. and Ficarella, A. (2023) 'Effects of battery degradation on a hybrid electric propulsive system management', *Int. J. Sustainable Aviation*, Vol. 9, No. 1, pp.41–57.

Biographical notes: Teresa Donateo is an Associate Professor of Fluid Machinery, Energy Systems, and Power Generation at the University of Salento since 2014, teaching courses on fluid machinery and hybrid-electric powertrains. She received her Master's in Materials Engineering from the Università degli Studi di Lecce, in 1999 and PhD in Combustion and Energy Conversion, in 2003 from ISUFI. Before completing her PhD, she joined the Faculty of Engineering at the University of Salento as an Assistant Professor. She has been collaborating since 2005 with the Ohio State University, Columbus, OH, since 2019 with the University of Brest, Brest, France, and since 2001 with major automotive and aircraft industrial partners. Author of more than 80 papers on simulation, design, and optimisation of internal combustion engines, fuel cells, electric and hybrid-electric powertrains for aircraft, heavy-duty vehicles, and passenger cars.

Ludovica Spada Chiodo received her Master of Science in Aerospace Engineering in 2021 and holds a research fellowship at the University of Salento.

Antonio Ficarella is a Full Professor of Energy and Environment Systems and the Director of the Department of Engineering for Innovation at University of Salento. He is a member of the Committee for the Development of Aeronautic Industry since 2014 and a coordinator of several research projects in collaboration with major industrial partners. In 1986, he took his Master of Science in Mechanical Engineering at the University of Bari, Italy and in 1992, he received his PhD in Mechanical Engineering at the University of Bologna, Italy. He is an author of more than 200 papers in the fields of energy, fluid machinery, environmental impact, and industrial plants.

This paper is a revised and expanded version of a paper entitled 'Influence of battery aging on energy management strategy' presented at International Symposium on Electric Aircraft and Autonomous Systems, Eskisehir, Turkey, 16–18 December 2021.

1 Introduction

The diffusion of hybrid powertrains in the field of small aviation is being largely encouraged by new advanced forms of air mobility that are getting increasing attention from aerospace manufacturers. A clear example is that of numerous aircraft concepts that are being developed for urban air mobility, which enable the application of electric and hybrid propulsive systems (Hill et al., 2020).

This emphasises the relevance of the management of such systems, which becomes a crucial aspect for their optimal usage considering that, amongst the most concerning issues regarding hybrid electric propulsive systems (HEPS), together with sizing and control, is that of energy management strategy (EMS) (Donateo et al., 2018b). In fact, according to Guzzella and Sciarretta (2007), supervisory control algorithms are designed to fulfil the power demand of the vehicle in the most convenient way, that is minimising the overall energy use.

According to Serrao (2009) the control problem in hybrid vehicles refers to the minimisation of the total cost, once a suitable optimisation horizon and cost function have been decided, using a sequence of instantaneous actions.

Such an issue has been extensively investigated in the automotive field, whose achievements serve as starting point for the research and the application of hybrid powertrains in the aeronautical field.

As for the control problem, the solution can be obtained with either numerical or analytical optimisation methods and with heuristic techniques. The first class includes dynamic programming (DP), which is one of the most common approaches to the problem in hybrid vehicles management. As an example, Pinto Leite and Voskuil (2020), apply DP to optimise fuel economy of a series-hybrid piston-prop light aircraft, while Bongermano et al. (2017) applied the same control algorithm to a parallel-hybrid UAV.

DP will be discussed later, since it has been employed here to obtain the reference discharge curve of the battery along the mission, which in turn is a baseline value

employed in the setting of the fuzzy logic (FL) rules. The proposed supervisory controller, therefore, follows a heuristic approach in determining the management strategy. Xie et al. (2019b) developed a FL controller for a hybrid piston-prop in parallel configuration for UAV application.

In fact, as stated in Lee et al. (2016), since the solution of the problem with DP cannot be performed in real-time unless a priori knowledge of the entire path is available, DP is often carried out offline to produce reference data that support the implementation of online control algorithms.

The present study focuses on the energy management of a parallel HEPS sized for a rotorcraft, made of a turboshaft engine coupled with two electric motors fed by a Li-ion battery.

The FL strategy employed here was developed by some of the authors in Donateo et al. (2021b) and is based on the derivation of an optimal battery discharge curve, carried out in Donateo et al. (2021a), with the objective of fuel consumption minimisation and the constraint of keeping the battery sufficiently charged, to ensure mission completion in case of engine failure. In fact, in the event of a single-engine failure, the aircraft could land safely if a sufficient amount of energy was still stored in the battery. So, the control laws on which the mission management strategy is based are designed by matching this constraint and will be discussed in the following.

Misley et al. (2021) developed a supervisory control based on a real-time application of Pontryagin minimum principle and compare it with a DP in a turboelectric system for commercial aviation.

Doff-Sotta et al. (2020) propose a model predictive control for a parallel hybrid turbofan to optimise fuel consumption while attaining battery SoC constraints and power limits both for the thermal and the electric machines and compares it with a common charge-depleting-charge-sustaining strategy.

The same approach is also employed by Zhang et al. (2022), where the authors validate the proposed method with an equivalent consumption minimisation strategy and evaluate potential fuel savings with different battery technology levels.

The central novel aspect of this study lies in the investigation of battery aging consequences on the vehicle EMS.

In fact, as underlined by Du et al. (2020), the development of a battery-aging aware energy management for HEVs is crucial for an optimal usage of the battery itself that avoids accelerated aging and thus shorter service life.

The need to update battery discharge profiles with battery age for PHEVs is also stated in Xie et al. (2019a), where the authors obtain the reference DoD through Pontryagin's minimum principle.

However, as also reported in Ebbesen et al. (2012), there is always a trade-off between fuel economy and battery preservation.

In particular, the aim of the present study is that of evaluating how a health-conscious strategy, that takes into account battery aging by varying its optimal discharge curve, will influence the global behaviour of the hybrid system along a typical mission, in particular in terms of fuel consumption and battery state of charge (SoC), especially in the perspective of flight safety as explained later. Two approaches will be compared on the same mission: one applies an age-dependent strategy, which adjusts the battery SoC threshold throughout its useful life to account for its gradual deterioration, while the

second approach sets the reference discharge as if battery performances were the same as at the beginning of its life, thus neglecting aging effects on this aspect.

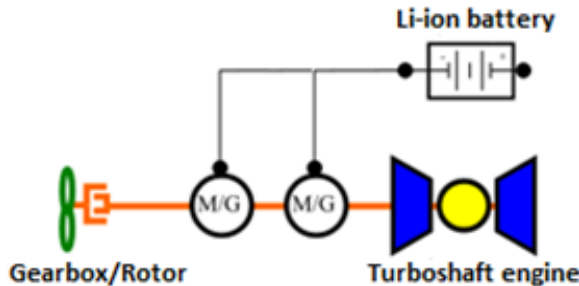
The paper is organised in this way. Section 2 describes the HEPS considered in this investigation and the reference mission while the detailed explanation of the modelling approach is reported in Section 3. Section 4 presents and discusses the results of the simulation.

2 The hybrid electric power system

The proposed study investigates the EMS set out by the supervisory controller in a HEPS in parallel configuration for aeronautical applications in presence of battery aging effects. According to Olsen and Page (2014), such configuration stems its superiority over series configuration thanks to the fact that only one electrical machine, namely a motor/generator, is needed, which can also be quite small if it is expected to work in power assist mode only. Moreover, the efficiency losses are significantly less than in series-hybrid. Thus, the non-optimal engine operation related to shaft speed constraint can be neglected if previously mentioned advantages are considered (Olsen et al., 2016).

The system is made of a turboshaft engine whose low-pressure spool is mechanically connected to a couple of two identical electric motors fed by a Li-ion battery (Figure 1). The output shaft, whose incoming torque is the algebraic sum of the engine output and the electric drive output, is ideally connected to a coaxial rotor for urban air mobility. Though, this aspect (i.e., the mechanical coupling device) is not dealt with at this stage, being a further development of the present study.

Figure 1 Scheme of parallel HEPS (see online version for colours)

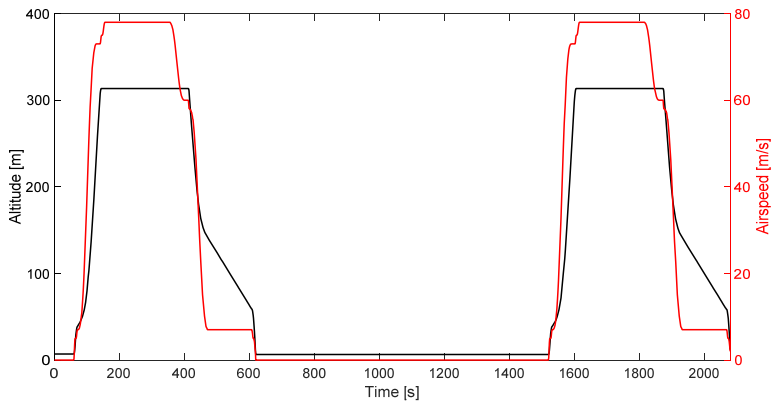


The size of the thermal engine has been selected to match the power demands of typical mission while the electric machines and the battery are sized for electric back-up operation in case of engine failure. The HEPS has a hybridisation degree (ratio of electric power to total installed power) of 0.45. The details of the machines and of the battery are not reported for the sake of confidentiality.

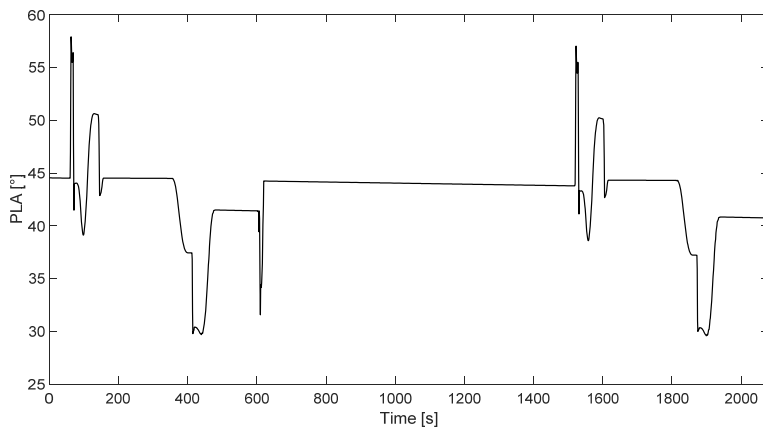
2.1 Reference missions

A typical mission of 2080s is considered for the rotorcraft on the basis of previous studies (Donateo et al., 2018a). The operating conditions, in terms of altitude, true airspeed (TAS) and power lever angle (PLA) command are shown in Figures 2(a) and 2(b).

Figure 2 (a) Mission altitude and airspeed (b) PLA variation during performed mission (see online version for colours)



(a)



(b)

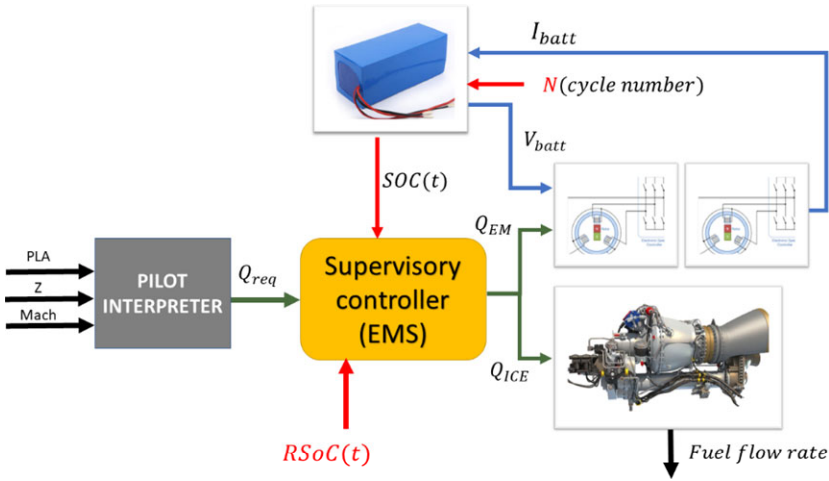
3 The simulation approach

The whole system is simulated in the MATLAB/Simulink environment as shown in Figure 3. A pilot interpreter block translates the PLA input into a power request, based on a 3D map which includes altitude and Mach effects. The resulting power request will be given in input to the supervisory controller, where the EMS is defined, as discussed in the next paragraph.

3.1 The turboshaft engine

The thermal engine is a two-spool turboshaft with a high pressure spool connecting compressor and high pressure turbine (HPT) and a low pressure turbine (LPT) delivering power to a low pressure spool and consequently to the rotor.

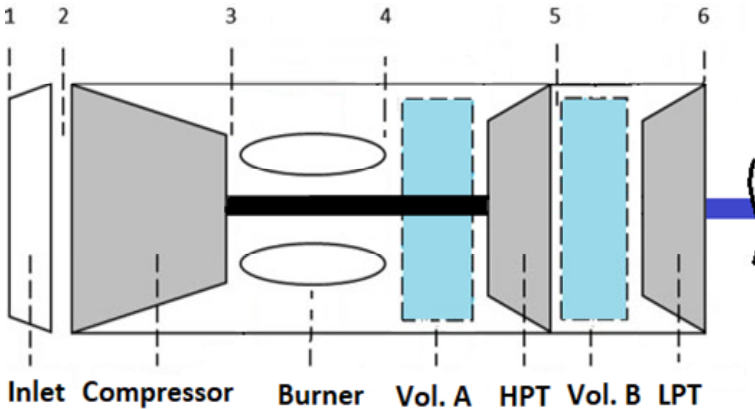
Figure 3 Flow chart of the simulation process (see online version for colours)



The air flows through the engine from a constant ram efficiency inlet which however determines a negligible pressure rise due to the typical low flight speeds.

The maps of each component (compressor map, HPT and LPT maps) have been obtained from the data available in the libraries of the GSP gas turbine simulation software and then implemented in the form of a lookup table in the Simulink model. An inter-component volume (ICV) has been applied to model the dynamic behaviour of the flow entering and leaving the HPT module (Figure 4), to account for non-stationary effects on mass flow rate during transient phases (Gaudet, 2007).

Figure 4 Scheme of turboshaft with ICVs (see online version for colours)



HP spool dynamics is modelled by applying a torque balance on the shaft, whose acceleration is therefore determined based on the mechanical inertia and the difference between the turbine torque output and the compressor torque request (Ballin, 1988). LP spool dynamic behaviour is neglected at the current stage since the shaft speed of the LPT and thus of the electric motors and the potential applied load is assumed constant here. The employed values of ICVs and HP shaft inertia have been derived from the

reference GSP model (Panov, 2009). Moreover, LPT exit pressure has been mapped on the basis of fuel flow rate with a correction to account for altitude effects.

The fuel flow rate is set by a PID controller acting on the LP turbine power error, whose parameters have been tuned through Simulink automated tuning tool. An accurate analysis of the LP shaft dynamics, as well as a proper design of fuel flow controller, is currently being investigated as further development by the authors.

3.2 The electric path

The electric motors are modelled through Simulink tool ‘Mapped Motor’ which implements mapped motor and drive electronics operating in torque control mode (MathWorks, n.d.). The output torque tracks the torque reference command and includes a default time constant for both the motor and drive dynamic response. The efficiency of the machine is mapped as a function of the required torque only, being the shaft speed constant in this case. The map of the motor allows obtaining required mechanical power and power losses and consequently calculating the value of battery current, given in input the voltage, as in equation (1):

$$I(t) = \frac{P_{mech} + P_{loss}}{V(t)} \quad (1)$$

Thus, an iterative procedure is required: in fact, the battery is modelled (with an in-house developed model) as an equivalent circuit with voltage $V(t)$ equal to:

$$V(t) = OCV - R_i \cdot I(t) \quad (2)$$

where OCV is the open circuit voltage mapped as a function of battery SoC as reported in many literature sources based on experimental SoC-OCV curves (Hasan et al., 2018; Yu et al., 2018) and R_i is the battery internal resistance, which will be updated with battery age as explained in the next section. The recourse to a R_{int} model is considered simple and effective for Li-ion batteries according to Wang et al. (2015), while higher complexity circuit models (as RC models) do not have analytical closed form solutions, as stated in Abdollahi et al. (2016).

The Peukert effect is included in the model in the following manner: an age-dependent Peukert coefficient n is considered to obtain the effective current I_{eff} as in equation (3):

$$I_{eff} = I \left(\frac{I}{I_{nom}} \right)^{n-1} \quad (3)$$

and hence calculate SoC with coulomb counting method as in equation (4):

$$SoC(t) = SoC(t_0) - 100 \cdot \int_{t_0}^t \frac{I_{eff}(t)}{C} dt \quad (4)$$

The employment of the coulomb counting method is suggested by several authors in the scientific literature, see for example Baccouche et al. (2018), where authors praise this method for its ease of implementation in contrast to model-based and data-oriented methods which require high computational complexity and big amount of data.

In equation (4), battery capacity is affected by battery age as explained in the following subsection.

3.3 Battery aging

Battery specification and model parameters are not constant since they change during battery life. The key aspects of battery deterioration can be identified in capacity fading and power fading. The causes of such mechanisms are to be ascribed to the increase of internal resistance and chemical modifications such as loss of electrolyte, loss of Li-ion inventory and loss of active material. These aspects are accurately discussed in Han et al. (2019) and their characterisation goes beyond the scope of this work.

As reported in Wang et al. (2011), time, temperature, depth of discharge (DoD) and discharge rate are among the most influential factors affecting capacity loss.

The reduction of nominal capacity together with an increase of the Peukert coefficient causes energy retention, while the power retention is associated mainly with the increase of the internal resistance. The open-circuit voltage is also affected by the battery cycle number.

The main specifications of the battery can be expressed as a function of the battery ‘cycle number’, which is defined as the number of complete discharge-recharge cycles. A battery is conventionally said to have reached its end of life (EoL) when the capacity reaches 80% of the nominal value. This usually happens, for a Li-ion battery, after 300–500 discharge-recharge cycles (Battery University, 2017).

The model employed here is based on the results of Dubarry and Liaw (2009), which experimentally characterised parameter variation over a LiFePO₄ battery life. On the basis of the above-mentioned research, some of the authors have developed the following equations for the dependence of battery parameters on cycle number N (Donateo and Ficarella, 2020): for each parameter P of the battery (namely nominal capacity C , Peukert coefficient n and internal resistance R_i), a correction factor related to battery age can be defined as follows:

$$CF = \frac{P(N)}{P^0} \quad (5)$$

where the superscript 0 denotes the initial condition.

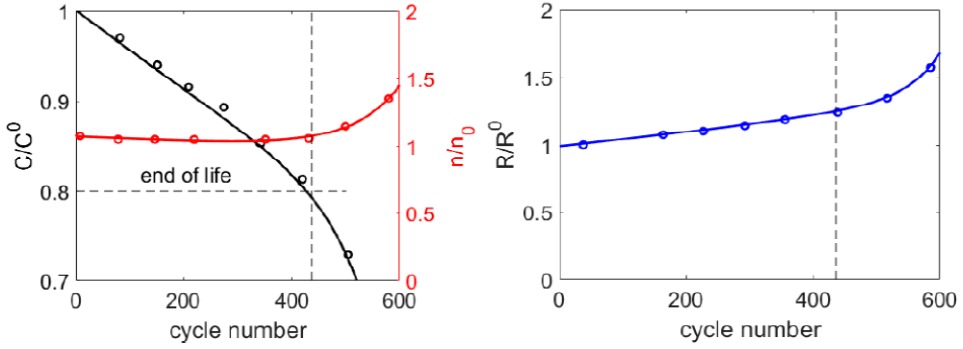
The dependence of the correction factor CF on battery cycle number N is expressed as a double exponential:

$$CF = a \cdot \exp(b \cdot N) + c \cdot \exp(d \cdot N) \quad (6)$$

where the coefficients a , b , c , d have been found interpolating experimental results from Dubarry and Liaw (2009) with least square error method. The fitting curves are depicted in Figure 5 together with experimental data. Since battery EoL is conventionally set to 20% capacity reduction with respect to the nominal value, the employed battery has a useful life of 436 cycles.

In the developed model, the battery state of health (SoH) is calculated as the ratio of undegraded internal resistance R_i^0 to current internal resistance $R_i(N)$ multiplied by a polynomial function of operating temperature.

Figure 5 Capacity, Peukert coefficient and internal resistance variation with battery age (see online version for colours)



3.4 Energy management strategy

The EMS is set by a supervisory controller based on fuzzy rules which consider power request, battery SoH and deviation of actual SoC from a reference state of charge (RSoC), which gives as output the power split k , defined as:

$$k = \frac{Q_{EM}}{Q_{req}} \quad (7)$$

where Q_{EM} is the torque load on the electric machines, while Q_{req} is the total required torque.

When SoH falls below 80%, the controller automatically reverts the strategy to only-thermal mode. Else, the controller distinguishes the strategy output in case of SoH higher or lower than 85%. In both cases, k is determined by a mapped function of the input parameters, resulting from the FL rules explained later. The maps stored in the supervisory controller were obtained in Donateo et al. (2021b).

The RSoC represents the ideal battery discharge obtained with the application of a DP algorithm in Donateo et al. (2021a) as follows: at first, the authors obtained the minimum allowable SoC threshold compatible with one engine inoperative (OEI) mission (Donateo and Ficarella, 2020). It was found that a new battery is able to perform the mission in only-electric mode as long as its SoC does not fall below 60%, while this threshold is raised to 70% at battery EoL. Such threshold values were obtained with the following procedure: the mission was simulated iteratively in only-electric mode, to represent an early engine failure scenario, lowering battery initial SoC at each iteration until battery SoC at the end of the mission was 20%, which can be considered the full-discharge value of such battery. This procedure was applied twice: at first on a new battery and then on a 400 cycle battery, resulting in the previously mentioned threshold values. This represented one of the constraints in the implementation of the DP, while the second constraint is that of equalling the total power output to the shaft request. The goal of the optimisation of the DP was the fuel saving with respect to the mission entirely run in only-thermal mode. The solution of the optimisation problem with k as control variable resulted in the so called RSoC, which represents the optimal battery discharge curve along the mission which satisfies the problem requirements.

Figure 6 Membership functions of FL inputs and outputs (see online version for colours)

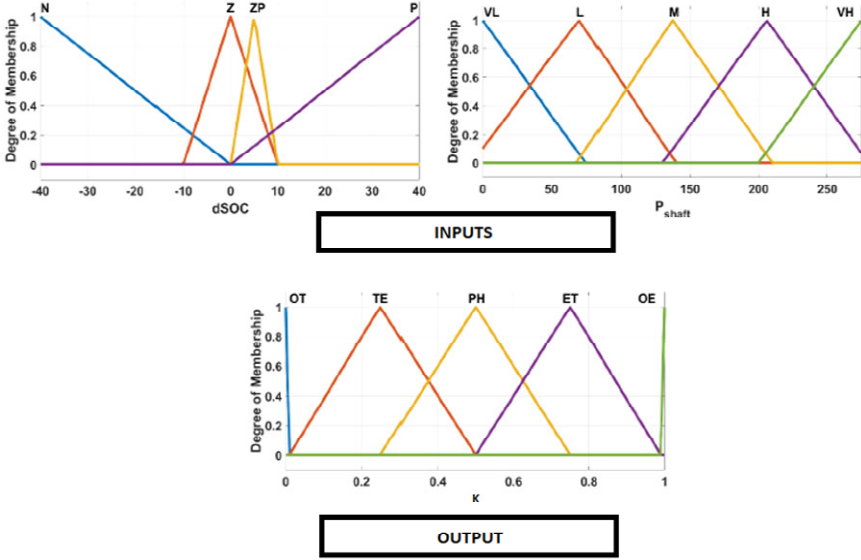
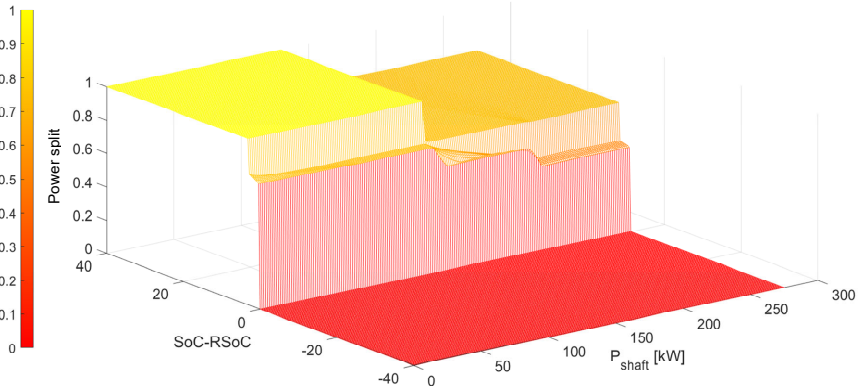


Figure 7 Map of FL supervisory controller output (see online version for colours)



Once this information became available, the FL supervisory controller has been implemented in Donateo et al. (2021b): an optimised triangular membership function is defined to classify the algorithm inputs, namely deviation of current SoC from RSoC at a given time instant and power request. The former, named deviation from reference SoC (dSoC), is classified in *negative*, *zero*, *zero-positive* and *positive*, while the latter is either *very low*, *low*, *medium*, *high* or *very high*. The membership degrees of both inputs are combined in *if ... and ... then* rules (Figure 6), which result in a 3D map of possible values of electric contribution, ranging from $k = 0$ (only-thermal) to $k = 1$ (only-electric), as shown in Figure 7. The classes of the output are the following:

- only-thermal
- thermal-electric, with an electric contribution lower than 25%

- thermal-electric, when the electric assist is as high as 50%
- electric-thermal, with an electric contribution until 75%
- only-electric.

Thus, the supervisory controller takes as input, at any time instant, $dSoC(t)$ and $P_{shaft}(t)$ and outputs k from its embedded maps. Then, the torque request on the engine (Q_{ICE}) and on the electric motors (Q_{EM}) are calculated as:

$$Q_{EM} = k \cdot Q_{req} \quad (8)$$

$$Q_{ICE} = (1 - k) \cdot Q_{req} \quad (9)$$

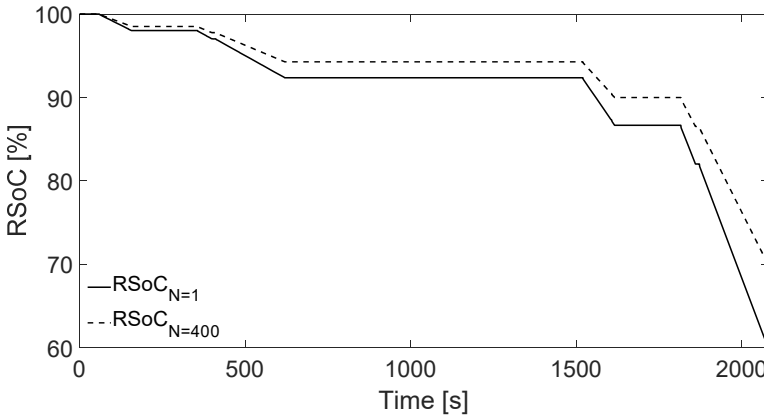
Note that, since the HEPS includes two electric motors on the electric path, the torque resulting from equation (8) is then equally subdivided between both.

Such FL algorithm was developed with MATLAB dedicated tool, while the membership function classes were previously optimised with a genetic algorithm in ModeFrontier, since mission fuel economy appeared very sensitive to their definition. For details, see Donato et al. (2021b).

As previously mentioned, two alternatives are implemented in the supervisory controller: one for $SoH > 85\%$ and one for $80\% < SoH < 85\%$: that is because the optimisation of the membership functions has been carried out twice, one for a new battery and one for a 400 cycle battery.

Moreover, two distinct RSoC curves were available after the implementation of DP with a new and an incipient EoL battery. The reference discharge curves are depicted in Figure 8. Note that the minimum allowable threshold needed to perform the mission in case of engine failure remains higher when the battery is deteriorated. In fact, as stated earlier, such constraint was previously obtained by running the mission in electric mode with both new and aged battery and resulted in a minimum allowed SoC of 60% for the new battery and 70% for incipient EoL battery to complete the mission safely.

Figure 8 RSoC for new and aged battery



At this point, a dual strategy has been tested: in one case, the RSoC is considered that of a new battery (solid line in Figure 8); in the second case, the RSoC is interpolated with battery age to comply with the effects of battery performance decay.

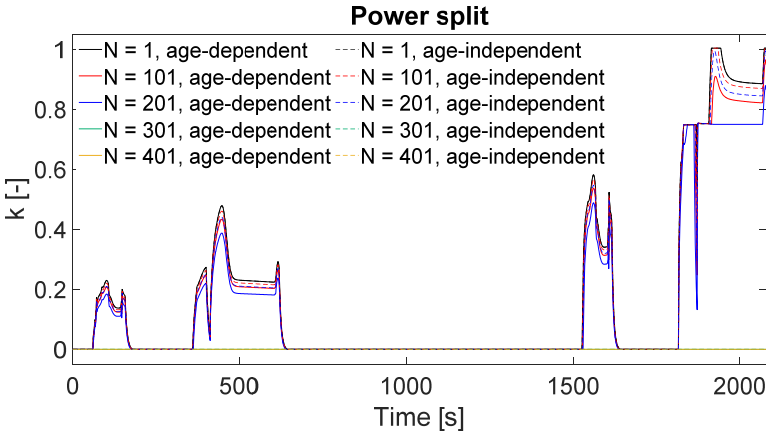
4 Results of the simulations

The previously discussed versions of mission EMS have been applied to the model running the same reference mission to highlight the differences due to inclusion of aging effects as primary constraint in the definition of the RSoC which, as it has been told before, underlies the implementation of the supervisory controller itself.

In particular, the analysis of the results focuses on global fuel consumption and battery DoD (equivalently SoC at the end of the mission), which can be regarded as the most valuable outputs from the mission optimisation standpoint.

At first, the supervisory controller output k is analyzed: the torque ratio of electric to total request resulting as output from the supervisory controller with both RSoC curves (either interpolated with battery age or typical of new battery), is depicted in Figure 9 on varying battery age every 100 cycles.

Figure 9 Influence of RSoC on mission electric contribution (see online version for colours)



Of course, the output of both strategies is the same when the battery is at the beginning of its life (black solid and dashed line are overlapped), while the strategy diverges in terms of recourse to the electric power source with increasing number of cycles: in fact, if battery deterioration is not neglected when determining reference discharge (age-dependent strategy), the supervisory controller will set a lower torque demand for the electric motors as long as battery age increases, at the expense of a higher recourse to thermal engine. In other words, the electric torque request is always lower when battery age is taken into account. Though, in the last 100 cycles of battery life, both strategies coalesce (green and orange lines, $k = 0 \forall t$). This happens because FL rules built in the supervisory controller take as input not only dSoC but also battery SoH, which is strongly deteriorated because of internal resistance increase (its initial value is slightly higher than 90% and drops to 75% after 400 cycles). The influence of SoH on the controller output also determines the gradual k decrease with increasing battery age for both strategies.

Next, the implications of these strategies in terms of fuel consumption and battery charge depletion will be analyzed.

Figure 10 shows the amount of fuel required to complete the simulated mission with both energy management approaches. Since k is always zero in the final stage of battery life ($N = 301$, $N = 401$), the fuel consumption in such cases represents the fuel

consumption of the pure-thermal propulsive system for the same mission, so it can be regarded as a benchmark value to compare with hybrid solutions results. On the contrary, the system hybridisation with a new battery follows exactly the strategy optimised in Donateo et al. (2021a), which allowed a fuel saving up to 11.7% with respect to the benchmark (only-thermal) value. During intermediate stages of battery life, a slight difference in fuel consumption is associated to both strategies, with a weak increase for the age-dependent strategy as expected, following from k adaptation to battery aging. Such increase is quite negligible during battery early life, becoming more evident with cycle number increase, as long as recourse to the thermal power source becomes higher (a maximum difference of 1.7% between the two strategies consumption can be observed at 251 cycles, before reversion to only-thermal configuration). However, it can be evinced how the worsening of battery SoH has a huge negative influence on fuel consumption, having caused the total exclusion of the electric machines from power generation when battery performance has become compromised.

Figure 10 Total fuel consumption per mission (see online version for colours)

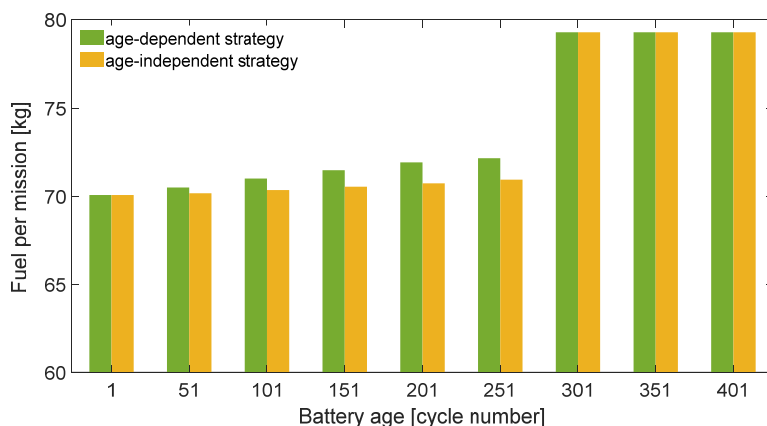
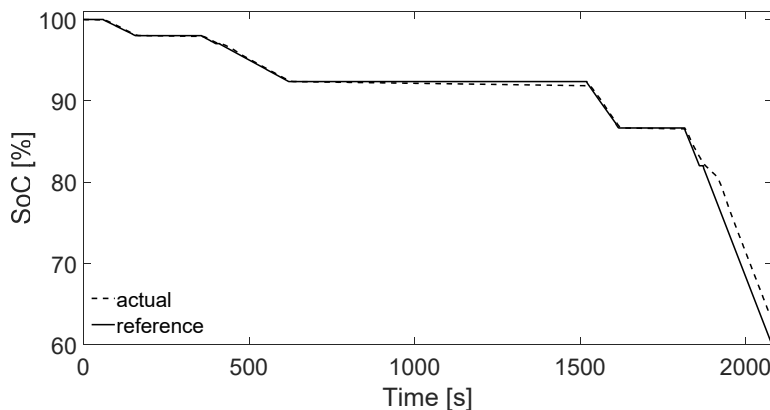


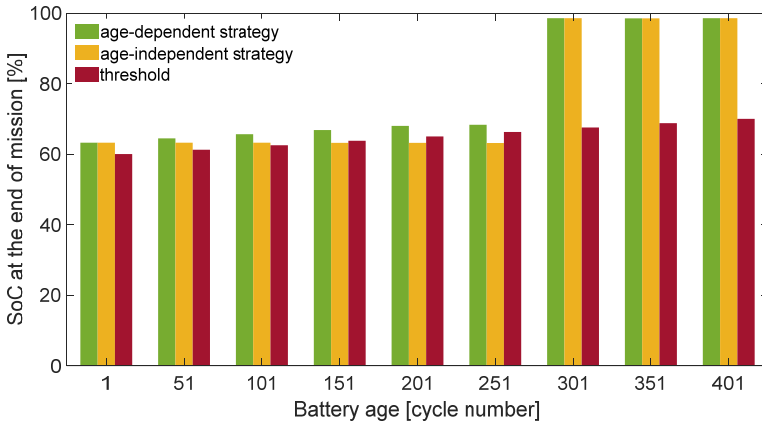
Figure 11 Battery discharge at first cycle (actual with respect to optimal)



Finally, the battery SoC at the end of mission is discussed. The baseline strategy, corresponding to the first cycle, determines a nearly optimal battery usage (close to the RSoC curve), leading to a final SoC almost equal to SoC threshold value (60%), as depicted in Figure 11.

Final SoC at different battery life stages with both energetic strategies is depicted in Figure 12. When battery aging is neglected in setting RSoC, k is only slightly altered, since in this case only SoH affects the mission management strategy: this implies that battery final SoC deviation from final $SoC_{N=1}$ is almost negligible, being the slight reduction in recourse to the electric power source cancelled out by battery simultaneous deterioration. Conversely, an age-dependent strategy determines a less aggressive battery usage, and hence a lower DoD as the battery degrades, to avoid an abusive employment of the battery that could eventually lead to safety constraint violation: in fact, it should be underlined that age-independent strategy does not guarantee that SoC minimum allowable threshold constraint is observed, being such approach insensitive to RSoC adaptation and thus unaware of progressive battery performance deterioration, in particular of its capacity loss. Thus, discharging the battery up to almost 60% independently of its age is not a safe usage, because the battery may not be able to perform an electric backup operation in case of engine failure. This may happen when applying the age-independent strategy with a battery older than 150 cycles, as it can be evinced from Figure 12 (final SoC falls below the safety threshold). Obviously, during the last cycles SoC remains unaltered at its initial value, being the electric motor not involved in power generation.

Figure 12 Battery SoC at mission completion (see online version for colours)



5 Conclusions

The increasing recourse to propulsive systems hybridisation in the field of small aviation highlights the need to develop suitable approaches to the issue of EMS, capable of dealing with effects of battery aging. In the present study, authors discussed the implications of battery aging on a previously developed FL algorithm for a parallel HEPS mission management: battery deterioration has been addressed by adapting the optimal battery discharge, calculated through a DP, so that the system could be able to complete

the mission safely if the turboshaft engine failed, also with an aged battery. The developed model simulates battery performance decay by mapping internal resistance and Peukert coefficient variation throughout battery life, to adjust SoC and SoH calculation with battery age. Such parameters, together with power request, serve as input to the FL supervisory controller, which determines power split between thermal and electric sources on the basis of the previously obtained RSoC. Two approaches have been compared, one which takes into account RSoC adaptation to battery age (age-dependent) and one which neglects such consideration (age-independent). In the latter case, the energy management would be affected only by the SoH decay, while in the former approach both RSoC and SoH influence combine, thus determining a more conservative strategy with regard to battery usage. This precaution allows the fulfilment of the safety constraint represented by a minimum SoC threshold compatible with an only-electric mission in case of engine failure, which has to be gradually updated to accommodate battery aging effects.

Since age-dependent strategy reduces recourse to electric motor torque with increasing cycle number, this results in slightly higher fuel consumption when such strategy is adopted. Though, it must be said that this increase is quite negligible, especially considering that minimum SoC level necessary to ensure electric backup could be violated by the age-independent strategy. Both strategies revert to only-thermal mode when the battery becomes too aged, because of prevailing SoH decay.

As a further development of the system dynamic model, LP spool dynamics will be characterised in detail, with the inclusion of a rotor dynamic model to assess system response to an actual set of pilot commands. A further improvement could be represented by the setting of a more accurate rpm governor.

Acknowledgements

This study has been funded by the Italian Ministry for Education, University and Research and developed in collaboration with Aerospace Technological District (DTA) and Avio Aero within project SMEA – Diagnostic and Prognostic Methods and Sensors Development for the Health Monitoring in Aeronautic and Transport Applications.

References

- Abdollahi, A. et al. (2016) ‘Optimal battery charging, part I: minimizing time-to-charge, energy loss, and temperature rise for OCV-resistance battery model’, *Journal of Power Sources*, Vol. 303, pp.388–398, <https://doi.org/10.1016/j.jpowsour.2015.02.075>.
- Baccouche, I. et al. (2018) ‘Implementation of an improved coulomb-counting algorithm based on a piecewise SOC-OCV relationship for SOC estimation of Li-ion battery’, *International Journal of Renewable Energy Research*, Vol. 8, No. 1, pp.178–187.
- Ballin, M. (1988) *A High Fidelity Real-Time Simulation of a Small Turboshaft Engine*, Moffett Field, CA, USA.
- Battery University (2017) *What is the Best Battery* [online] https://batteryuniversity.com/learn/archive/whats_the_best_battery (accessed September 2021).
- Bongermimo, E. et al. (2017) ‘Model and energy management system for a parallel hybrid electric unmanned aerial vehicle’, *Proceedings of 2017 IEEE 26th International Symposium on Industrial Electronics (ISIE)*, Edinburgh, UK, DOI: 10.1109/ISIE.2017.8001534.

- Doff-Sotta, M., Cannon, M. and Bacic, M. (2020) 'Optimal energy management for hybrid electric aircraft', *IFAC-PapersOnLine*, Vol. 53, No. 2, pp.6043–6049.
- Donateo, T. and Ficarella, A. (2020) 'A modeling approach for the effect of battery aging on the performance of a hybrid electric rotorcraft for urban air-mobility', *Aerospace*, Vol. 7, No. 5, Article No. 56, DOI: 10.3390/aerospace7050056.
- Donateo, T., Carlà, A. and Avanzini, G. (2018a) 'Fuel consumption of rotorcrafts and potentiality for hybrid electric power systems', *Energy Conversion and Management*, Vol. 164, pp.429–442, DOI: <https://doi.org/10.1016/j.enconman.2018.03.016>.
- Donateo, T., De Pascalis, C. and Ficarella, A. (2018b) 'Exploiting the synergy between aircraft architecture and electric power system in unmanned aerial vehicle through many-objective optimisation', *International Journal of Sustainable Aviation*, Vol. 4, Nos. 3/4, pp.247–272.
- Donateo, T., De Pascalis, C., Strafella, L. and Ficarella, A. (2021a) 'Off-line and on-line optimization of the energy management strategy in a hybrid electric helicopter for urban air-mobility', *Aerospace Science and Technology*, Vol. 113, Article No. 106677, DOI: <https://doi.org/10.1016/j.ast.2021.106677>.
- Donateo, T., Terragno, A. and Ficarella, A. (2021b) *An Optimized Fuzzy Logic for the Energy Management of a Hybrid Electric Air-Taxi*, No. 76, Italian National Congress, ATI.
- Du, R. et al. (2020) 'Battery aging- and temperature-aware predictive energy management for hybrid electric vehicles', *Journal of Power Sources*, Vol. 473, Article No. 228568, DOI: <https://doi.org/10.1016/j.jpowsour.2020.228568>.
- Dubarry, M. and Liaw, B. (2009) 'Identify capacity fading mechanism in a commercial LiFePO₄ cell', *Journal of Power Sources*, Vol. 194, No. 1, pp.541–549, DOI: <https://doi.org/10.1016/j.jpowsour.2009.05.036>.
- Ebbesen, S., Elbert, P. and Guzzella, L. (2012) 'Battery state-of-health perceptive energy management for hybrid electric vehicles', *IEEE Transactions on Vehicular Technology*, Vol. 61, No. 7, pp.2893–2900.
- Gaudet, S. (2007) *Development of a Dynamic Modeling and Control System Design Methodology for Gas Turbines*, Ottawa, Canada.
- Guzzella, L. and Sciarretta, A. (2007) *Vehicle Propulsion Systems: Introduction to Modeling and Optimization*, Springer, Berlin, Germany.
- Han, X. et al. (2019) 'A review on the key issues of the lithium ion battery degradation among the whole life cycle', *eTransportation*, Vol. 1, Article No. 100005, DOI: <https://doi.org/10.1016/j.etrans.2019.100005>.
- Hasan, A., Skriver, M. and Johansen, T. (2018) 'eXogenous Kalman filter for state-of-charge estimation in lithium-ion batteries', *Proceedings of 2018 IEEE Conference on Control Technology and Applications (CCTA)*, Copenhagen, Denmark, DOI: 10.1109/CCTA.2018.8511577.
- Hill, B.P. et al. (2020) *UAM Vision Concept of Operations (ConOps) UAM Maturity Level (UML) 4*, Document ID 20205011091, NASA.
- Lee, H., Kang, C., Park, Y-i. and Cha, S. (2016) 'Study on power management strategy of HEV using dynamic programming', *World Electr. Veh. J.*, Vol. 8, No. 1, pp.274–280.
- MathWorks (n.d.) *Mapped Motor* [online] <https://www.mathworks.com/help/autoblks/ref/mappedmotor.html> (accessed March 2022).
- Misley, A., D'Arpino, M., Ramesh, P. and Canova, M. (2021) 'A real-time energy management strategy for hybrid electric aircraft propulsion systems', *AIAA Propulsion and Energy 2021 Forum*.
- Olsen, J. and Page, J. (2014) 'Hybrid powertrain for light aircraft', *International Journal of Sustainable Aviation*, Vol. 1, No. 1, pp.85–102.
- Olsen, J., Page, J. and Vulovic, Z. (2016) 'Alternative energy storage and energy harvesting methods for parallel hybrid light aircraft', *Int. J. Sustainable Aviation*, Vol. 2, No. 2, pp.128–148.

- Panov, V. (2009) *GasTurboLib: Simulink Library for Gas Turbine Engine Modelling*, ASME, Orlando, FL, USA, pp.555–565.
- Pinto Leite, J. and Voskuil, M. (2020) ‘Optimal energy management for hybrid-electric aircraft’, *Aircraft Engineering and Aerospace Technology*, Vol. 92, No. 6, pp.851–861.
- Serrao, L. (2009) *A Comparative Analysis of Energy Management Strategies for Hybrid Electric Vehicles*, PhD thesis, The Ohio State University.
- Wang, J. et al. (2011) ‘Cycle-life model for graphite-LiFePO₄ cells’, *Journal of Power Sources*, Vol. 196, No. 8, pp.3942–3948.
- Wang, X., Hongwen, H., Sun, F. and Zhang, J. (2015) ‘Application study on the dynamic programming algorithm for energy management of plug-in hybrid electric vehicles’, *Energies*, Vol. 8, No. 4, pp.3225–3244, DOI: <https://doi.org/10.3390/en8043225>.
- Xie, S. et al. (2019a) ‘Model predictive energy management for plug-in hybrid electric vehicles considering optimal battery depth of discharge’, *Energy*, Vol. 173, pp.667–678, <https://doi.org/10.1016/j.energy.2019.02.074>.
- Xie, Y., Savvaris, A. and Tsourdos, A. (2019b) ‘Fuzzy logic based equivalent consumption optimization of a hybrid electric propulsion system for unmanned aerial vehicles’, *Aerospace Science and Technology*, Vol. 85, pp.13–23, DOI: <https://doi.org/10.1016/j.ast.2018.12.001>.
- Yu, Q., Xiong, R., Wang, L. and Lin, C. (2018) ‘A comparative study on open circuit voltage models for lithium-ion batteries’, *Chinese Journal of Mechanical Engineering*, Vol. 31, Article No. 65, DOI: <https://doi.org/10.1186/s10033-018-0268-8>.
- Zhang, J., Roumeliotis, I. and Zolotas, A. (2022) ‘Nonlinear model predictive control-based optimal energy management for hybrid electric aircraft considering aerodynamics-propulsion coupling effects’, *IEEE Transactions on Transportation Electrification*, Vol. 8, No. 2, pp.2640–2653.

Nomenclatures

DoD	Depth of discharge
DP	Dynamic programming
dSoC	Deviation from reference SoC
EoL	End of life
FL	Fuzzy logic
HEPS	Hybrid electric propulsive system
HPT	High pressure turbine
LPT	Low pressure turbine
OEI	One engine inoperative
PLA	Power lever angle
RSoC	Reference state of charge
SoC	State of charge
SoH	State of health
TAS	True airspeed
